Journal of Materials Chemistry

Cite this: *J. Mater. Chem.*, 2012, **22**, 12915

www.rsc.org/materials

PAPER

Study on formaldehyde gas-sensing of In_2O_3-sensitized ZnO nanoflowers under visible light irradiation at room temperature†

Lina Han, Dejun Wang, Jiabao Cui, Liping Chen, Tengfei Jiang and Yanhong Lin*

Received 23rd November 2011, Accepted 1st May 2012
DOI: 10.1039/c2jm16105b

In_2O_3-sensitized flowerlike ZnO with visible light photoelectric response properties were synthesized by a facile two-step process, and characterized by X-ray diffraction (XRD), scanning electron microscopy (SEM), EDAX, HRTEM and UV-vis diffuse reflectance spectroscopy. The results revealed that In_2O_3 nanoparticles have grown and eventually coalesced on the surface of the flowerlike ZnO successfully, and the samples exhibited significant response to visible light. The photoelectric gas-sensing of the In_2O_3-sensitized ZnO was also studied to formaldehyde (HCHO) under 460 nm light irradiation at room temperature with the help of surface photocurrent technique. It was found that ZnO sensitized with In_2O_3 could enhance the gas response to HCHO under the visible light illumination. This may be due to the fact that the composite structure of In_2O_3–ZnO extends the photo absorbing range to visible light area, inhibits the recombination of photo-generated electrons and holes, and thus increases the utilization of photo-generated carriers in photoelectric gas detection, resulting in the higher sensing response in some extent. The gas response to 5 ppm and 100 ppm formaldehyde can reach to 19% and 419% under visible light irradiation at room temperature, respectively. These results should be valuable for designing a new type of visible-light assisted gas sensor at room temperature.

1. Introduction

Semiconductor metal oxide (MOS) gas sensors have been widely used in process control industries,[1] medical and environmental diagnostics[2] and public safety.[3,4] However, the traditional heat-treatment gas sensors have to be operated at high temperatures in order to exhibit their sensing behavior. These operating conditions are highly inconvenient for practical applications and do not fulfil the requirements of the market.[5,6] Recently, many reports proved that light illuminating gas sensors are a viable alternative to activating chemical reactions at room temperature,[7–10] which would significantly reduce explosion hazards, and improve device lifetime and sensitivity.

Zinc oxide (ZnO),[11] with a wide band gap of 3.37 eV, has been considered as one of the promising materials in the field of gas sensors for organic pollutants under UV light irradiation.[12–15] For example, Peng *et al.* successfully synthesized ZnO nanoribbons,[16] ZnO nanorods,[17] co-doped ZnO,[18] ZnO modified with $Ru(dcbpy)_2(NCS)_2$ (ref. 19) and detected O_2, H_2O, HCHO, CH_3CH_2OH respectively under ultraviolet (UV) light irradiation. ZnO/SnO_2,[20] TiO_2-doped ZnO[21] and so on were also synthesized to detect NO_2 and CH_3CH_2OH with UV light irradiation, respectively. However, compared to the UV light region, there is much more energy which is produced by the sunlight in the visible light region.[17] Therefore, in order to extend the photoelectric response of wide band gap semiconductors into the visible spectral range and utilize solar energy effectively, various methods have been attempted.[18–26] Among them, the composite system incorporating a narrow band gap semiconductor which served as the sensitizer has been demonstrated as an efficient attempt to absorb visible light.[27,28] Although the narrow band gap semiconductors exhibit a good absorbance to visible light, they usually suffer from several critical limitations such as relatively low sensitivity and poor selectivity due to the recombination of photo-generated electrons and holes. Recently, many reports demonstrated that composite system can improve the photoelectric activity under visible light irradiation, such as CdS–ZnO,[27] Zn–Al–In,[29] silicon–polymer,[30] ZnO–TiO_2[31] and polypyrrole–TiO_2–ZnO.[32] The reason is that the composite can compensate for the disadvantages of the individual component, inhibit recombine of photo-generated electrons and holes, and thus improve sensitivity.

Among a variety of semiconductor sensitizers, In_2O_3 (ref. 33) with an indirect band gap of 2.56 eV which has an excellent electric conductance, transparency to visible light, and good stability can be one of the ideal sensitizers used for ZnO due to the appropriate location of conduction and valence band gap position.[34,35] The In_2O_3–ZnO composite system had already been fabricated by various methods and was applied in flat-panel displays, light-emitting diodes, and thin film transistors, *etc.*[36–38] Recently, the photocatalytic properties of In_2O_3–ZnO composite have been

College of Chemistry, Jilin University, Changchun 130012, People's Republic of China. E-mail: linyh@jlu.edu.cn; Tel: +86 0431 85168093
† Electronic supplementary information (ESI) available. See DOI: 10.1039/c2jm16105b

reported. Zhou *et al.*[39] synthesized In_2O_3-sensitized ZnO nanowire (NW) array film and investigated the photocatalytic activity by the oxidation of glucose under visible light irradiation. Wang *et al.*[40] synthesized In_2O_3–ZnO heteronanostructures by a co-precipitation method and evaluated the photocatalytic activities of the In_2O_3–ZnO heteronanostructures by the bleaching of MB dye under the irradiation of a Xe arc lamp. The results above showed that the incorporation of In_2O_3 in ZnO nanostructure remarkably promotes the photo-generated carrier separation, increases the utilization of photo-generated carriers and enhances the photocatalytic activity. However, to the best of our knowledge, the visible-light assisted gas-sensing properties of the In_2O_3–ZnO composite system have never been reported. In addition, a conventional semiconductor gas sensor can alter its resistance by alteration of its temperature so as to detect gas.[41–43] In contrast, the surface photocurrent technique is an effective method to study the changes of the conductance on the surface or at interfaces caused by the illumination.[14,27] This change can be shown by the corresponding surface photocurrent response. Importantly, what is reflected from the information obtained by the method is the character of the surface layers rather than that of the substrates. Therefore, the surface photocurrent response is very sensitive to the change of photoelectric properties of materials aroused by the gas absorption. It is well known that the surface and interface state of sensitive materials are key factors that affect the performances of the sensors.[27] Considering the excellent photoelectric properties of In_2O_3–ZnO composite system and the gas detection technique based on surface photocurrent response,[18] we have full reason to believe that this promising structure will realize the enhanced visible-light assisted photoelectric gas-sensing at the room temperature.

It is well known that the gas response is also influenced by the morphology. Although nanoparticles have a smaller size, a high gas response cannot be achieved because of the aggregation between the nanoparticles are very strong. The 1D nanostructures such as nanowires, nanorods with a less agglomerated configuration, have been used to improve gas-sensing characteristics. Recently many reports have shown that the flower-like samples have better photoelectric properties.[44,45] Therefore, in this work, we synthesized In_2O_3-sensitized flowerlike ZnO by a facile two-step process and investigated its sensing properties to HCHO under visible light irradiation by means of a surface photocurrent technique. It was found that the gas sensitivity of the In_2O_3-sensitized ZnO has been enhanced significantly compared with pure ZnO. The effects of In_2O_3 on the sensing mechanism of In_2O_3-sensitized ZnO nanoflowers were investigated. This work may support fundamentals for gas-sensing of In_2O_3-sensitized ZnO nanoflowers dependent on surface photocurrent at room temperature.

2. Experimental section

2.1. Synthesis of In_2O_3-sensitized flowerlike ZnO

All chemicals were analytical-grade reagents used in the as-received condition, without any further purification. The synthesis of the flowerlike In_2O_3-sensitized ZnO was prepared by a facile two-step process: synthesized of ZnO nanoflowers and coating with In_2O_3. Firstly, ZnO nanoflowers were synthesized according to the previous report.[46] 4 mmol (0.878 g) $Zn(CH_3COO)_2 \cdot 2H_2O$ were put into 60 mL water, stirred at room temperature for 5 min, and then 20 mL of 3 M NaOH aqueous solution were introduced into the above solution, respectively. After the mixture was stirred magnetically for 10 min, the solution was moved to 100 mL Teflon-lined stainless steel autoclaves, sealed and maintained at 150 °C for 10 h. When the reactions were completed, the autoclave was cooled down to room temperature naturally. The white products were filtered off, and washed with de-ionized water two times to remove possible impurities. Secondly, depositing of In_2O_3 on ZnO nanoflowers. 0.048 g $In(NO_3)_3$ was mixed with 200 mL water to form $In(OH)_3$ aqueous solution. Then the as-prepared products were washed with 20 mL $In(NO_3)_3$ aqueous solution once, twice and three times, respectively. The precipitates were dried at ambient air at 60 °C for 10 h and then sintered at 600 °C for 2.5 h to get a series of In_2O_3-sensitized ZnO powders labled ZNFI-1, ZNFI-2 and ZNFI-3. Meanwhile, pure ZnO sample was also synthesized using an identical procedure for comparison.

2.2. Characterization of In_2O_3-sensitized ZnO

XRD patterns of the In_2O_3-sensitized ZnO was obtained by X-ray diffraction (XRD) (Rigaku D/Max-2550, Cu Kα λ = 1.54056 Å) measurement. SEM of the In_2O_3-sensitized ZnO was obtained with scanning electron microscopy (Shimadzu, SS-550). HRTEM of the In_2O_3-sensitized ZnO nanoflowers was obtained with TECNAIG^2 microscope (FEI company). A UV-vis spectrophotometer (UV-3600) was employed to obtain the diffuse reflectance spectra of the samples. Surface photocurrent was measured with self-made instrument,[47] which was composed of a source of monochromatic light, a lock-in amplifier (SR830-DSP) with a light chopper (SR540), an electrochemistry workstation (CHI 630b, made in China), a sample cell and a computer. The monochromatic light was obtained by the double-prism monochromatic (Hilger and Watts, D300 made in England) and a 500 W xenon lamp (CHFXQ500 W, Global xenon lamp power, China), and the electrochemistry workstation system was used to (CHI600, China) record the current intensity with the bias voltage of 10 V.

2.3. Gas-sensing measurement

Gas-sensing properties were measured based on the SPC measurement which included a test chamber and an electrochemistry workstation system. The sensor was fabricated by putting the powder on a comb-like indium doped tin oxide (ITO) transparent electrode and then put into the test chamber. HCHO liquid was injected into the test chamber by a syringe through a rubber plug. Air was used both as a reference gas and a diluting gas to obtain desired concentrations of HCHO. HCHO was injected into the test chamber by a syringe. After HCHO was fully mixed with the air gas, the sensor was illuminated by light. The light was blocked when the sample illustrated by light with a certain period of time. An electrochemistry workstation (CHI 630b, made in China) was used to record the current intensity across the gas sensor with a bias voltage of 10 V. Monochromatic light (460 nm, 0.213 mW cm^{-2}) was obtained by a monochromator (Hilger and Watts, D300 made in England), and the

light source was a Xe-lamp (CHF-XQ500W, Global xenon lamp power made in China). The light can irradiate the sensor through a quartz window of the test chamber. In this measurement, the vapor concentration of HCHO was calculated according to our groups' previous research.[48] In addition, all the measurements were taken at room temperature.

3. Results and discussion

3.1. Morphologies structures

The XRD patterns for ZnO and In_2O_3-sensitized ZnO are shown in Fig. 1, which provide further insight into the crystallinity of the products. From Fig. 1, it is clear that the sample ZNF shows a pure phase of ZnO. With the increasing washed times with $In(NO_3)_3$ aqueous solution, the diffraction peaks corresponding to (2 1 1), (2 2 2), (4 0 0), (4 4 1), (3 3 2), (4 3 1), (4 4 0), (5 4 1) and (6 2 2) reflections of In_2O_3 are much more evident, and no peak shifts or any trace of mixed metal compounds can be detected. It implies that our samples are considered to be mainly composed by ZnO and In_2O_3 with separate phases. Compared with pure ZnO, these additional XRD peaks correspond to In_2O_3 are marked by stars.

The morphology of pure ZnO and In_2O_3-sensitized ZnO was characterized by scanning electron microscopy. As shown in Fig. 2, the samples are self-assembled from nanorods with the lengths of 3–3.5 μm and diameters of 350–450 nm. It can be clearly seen from the images that the surface of the original nanoflowers is smooth. However, after washing with the $In(NO_3)_3$ aqueous solution, the rods are coarser than those of pure ZnO. Besides that, we can see from Fig. 2(d), (f) and (h) that there are many In_2O_3 nanoparticles on the surface of the ZnO nanoflowers, and the amount of In_2O_3 nanoparticles increased with the increasing washed time. Only Zn and O atoms were detected in the energy-dispersive X-ray spectroscopy (EDAX) of the pure ZnO nanoflowers, whereas the In_2O_3-sensitized ZnO nanoflowers shows Zn and O in addition to In (Fig. 2(i) and (j)). And the ratio of In element is 1.06 mol%, which is consistent with the theoretical value. Considering the results of SEM, EDAX and XRD, we deduced that the In_2O_3 nanoparticles have grown and eventually coalesced on the surface of the ZnO nanorods. Besides that, it can be seen from Fig. 2 that the morphology of ZnO is unspoiled when In_2O_3 are deposited.

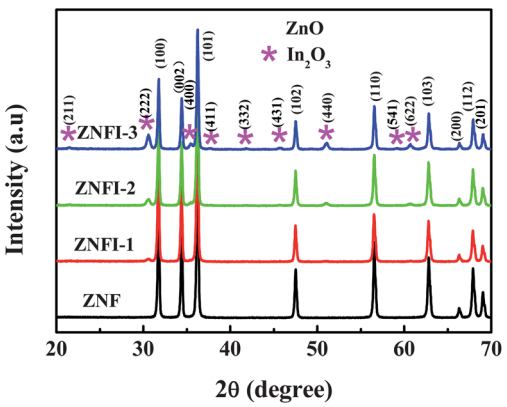

Fig. 1 XRD patterns of ZnO and In_2O_3-sensitized ZnO nanoflowers.

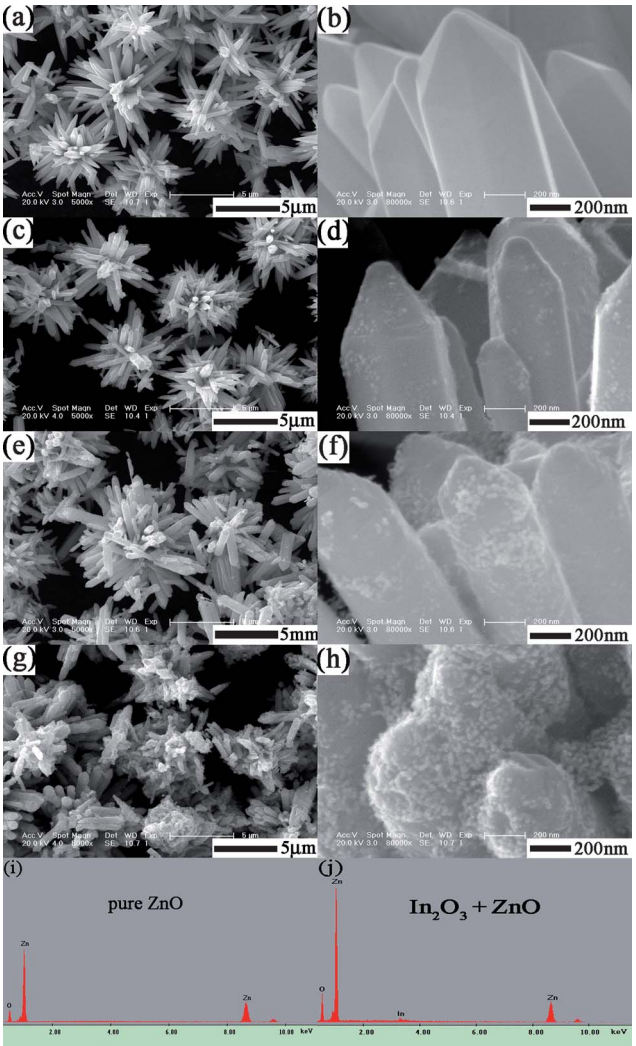

Fig. 2 SEM images of ZnO and In_2O_3-sensitized ZnO nanoflowers: (a and b) pure ZnO nanoflowers, (c and d) ZNFI-1, (e and f) ZNFI-2, (g and h) ZNFI-3, (i and j) energy-dispersive X-ray spectroscopy (EDAX) recorded from pure ZnO nanoflowers and In_2O_3-sensitized ZnO nanoflowers, respectively.

In order to obtain detailed information about the nanostructure and morphology of the as-synthesized samples, the HRTEM images of In_2O_3-sensitized ZnO nanoflowers is performed, as is shown in Fig. 3. From the TEM images shown in Fig. 3(a) and (b), we can see that the ZnO nanoflowers surface is uniformly coated with many In_2O_3 nanoparticles of thickness 20–40 nm. The high-resolution images of the ZnO–In_2O_3 interface region indicate that the In_2O_3 nanoparticles were deposited on the single crystalline hexagonal ZnO nanowires grown along the *c*-axis. From the magnified image In_2O_3-sensitized ZnO nanorods shown in Fig. 3(c) (square region marked in Fig. 3(b)), the lattice structure of In_2O_3 was identified with a (200) interplanar spacing of 0.26 nm. Also, in another region (the round region marked in Fig. 3(b)), an In_2O_3 (211) spacing of 0.413 nm was recognized. These results also suggest that the as-synthesized sample behaved as a well-crystallized sample with the In_2O_3 nanoparticles and ZnO nanorods on the nanoscale, which is

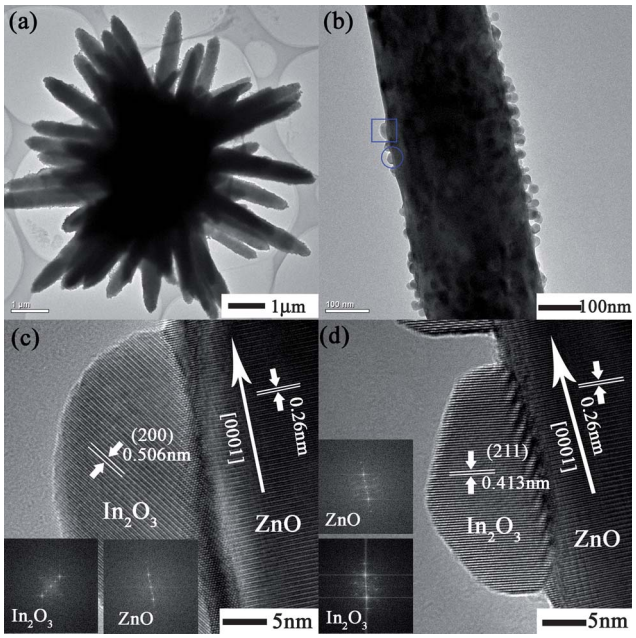

Fig. 3 HRTEM images of In_2O_3-sensitized ZnO nanoflowers (ZNFI-2): (a) TEM image of In_2O_3-sensitized ZnO nanoflower (ZNFI-2); (b) a typical TEM of a single In_2O_3-sensitized ZnO nanorod; (c and d) the high resolution TEM images of In_2O_3 nanoparticles and ZnO nanorods, inset shows the corresponding fast-Fourier transform (FFT).

propitious for electron transmission between In_2O_3 nanoparticles and ZnO nanorods.

3.2. UV-vis reflectivity spectra

In order to study the optical properties of the In_2O_3-sensitized ZnO, the UV-vis DRS characterization is performed, as is shown in Fig. 4. From Fig. 4, it can be seen that the pure ZnO shows a clear absorption edge at around 403 nm (3.08 eV). Meanwhile, compared with pure ZnO, the optical response of In_2O_3-sensitized ZnO samples has a red shift toward the longer wavelength region, and the absorption intensities between 400 and 500 nm are raised up. These results can be attributed to the existence of In_2O_3 and the formation of the In_2O_3–ZnO composite system. From Fig. 2, it can also be seen that the amount of In_2O_3 in the sample increasing with the increasing washed time, which is the same as the conclusion of the XRD. Importantly, the red-shift of optical absorption further confirmed that In_2O_3–ZnO composite has an effective absorption for visible light, which is a key factor in the visible-light-induced photoelectric gas-sensing.

3.3. Gas-sensing performance

The surface photocurrent spectra of the In_2O_3-sensitized ZnO are displayed in Fig. 5. It is clearly seen that the photocurrent intensity is increased dramatically, and the response range of photocurrent is extended to 500 nm with the corporation of In_2O_3. Besides that, the photocurrent intensity increased gradually with the increasing amount of In_2O_3. The results indicated that In_2O_3 can enhance the surface photocurrent response intensity as well as extend the photocurrent response range of ZnO nanomaterials to the visible region. These results are very important for the achievement of visible-light-assisted gas-sensing. In addition, according to the surface photocurrent spectra, the 460 nm light was selected as irradiation light for sensing measurement. The main reason for this is that the sensitized samples exhibit the obvious photocurrent response at this wavelength compared with the pure ZnO, and as well as the gas detection under 460 nm light illumination can reduce the impact of the photo-generated electron which produced by intrinsic excitation of ZnO.

In order to test the photo-response and stability of the samples for irradiation light, the five cycles experiments were carried out with and without 460 nm light illumination. The experimental results are shown in Fig. 6. From the Fig. 6, it can be seen that the photocurrent increased rapidly under 460 nm light irradiation. The photocurrent intensities are about 3.0 μA, 0.035 mA, 0.051 mA and 0.087 mA in ZNF, ZNFI-1, ZNFI-2 and ZNFI-3, respectively. Due to the special position of the valance band and conducting band between ZnO and In_2O_3,[49] the coupling effects of ZnO and In_2O_3 as a kind of heterostructure will take place. When the samples were illuminated by 460 nm light, the In_2O_3 coating on the wall of flowerlike ZnO effectively absorbs visible light and produces photo-generated electrons. The electron at the conducting band bottom of In_2O_3 would migrate to the conducting band of ZnO. In this way, the recombination of

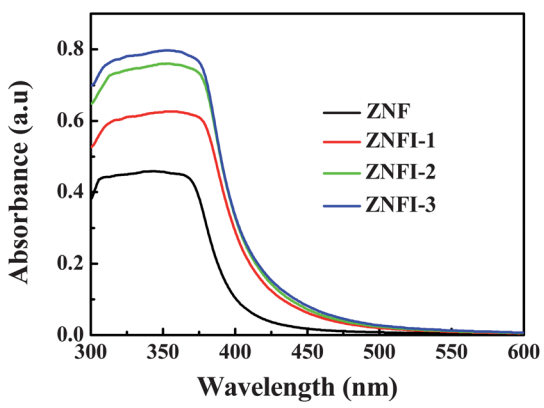

Fig. 4 UV-vis diffuse reflectance spectra of the ZnO and In_2O_3-sensitized ZnO nanoflowers.

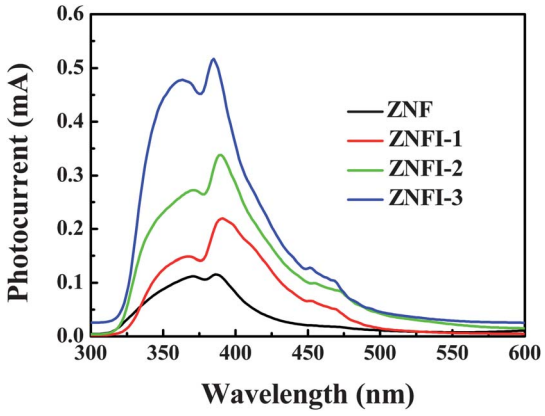

Fig. 5 Photocurrent spectra of the ZnO and In_2O_3-sensitized ZnO nanoflowers with a bias voltage of 10 V.

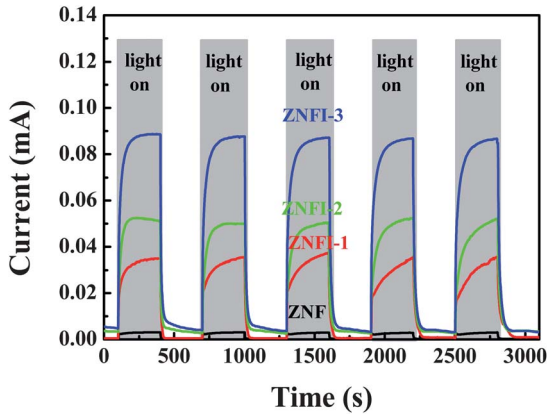

Fig. 6 Surface photocurrent of the ZnO and In_2O_3-sensitized ZnO nanoflowers exposed to five cycles of light on–off with a bias voltage of 10 V under 460 nm light illumination.

photo-generated holes and electrons in In_2O_3-sensitized ZnO nanomaterials is inhibited, which effectively improves the carrier separation efficiency. Furthermore, with the quantity of In_2O_3 nanoparticles increases, more photo-generated electrons can be injected into ZnO. Therefore, the samples of In_2O_3-sensitized ZnO exhibit the highest photocurrent response among all our samples. However, in the absence of light, due to photo-generated electrons and holes recombination on the surface, the number of free-electrons decreases. Therefore, the photocurrent intensity decreases obviously and the recovery time are less than 30 s. More importantly, the photocurrent response did not change after five cycles experiments. It is demonstrated that ZnO sensitized with In_2O_3 is not prone to light poisoning, light corrosion and photodegradation itself under 460 nm light irradiation, and it is a suitable candidate material for photoelectric gas sensors.

The gas-sensing properties of the samples for formaldehyde were measured under 460 nm light irradiation at room temperature. The response curves of sensor to different concentrations of formaldehyde are shown in Fig. 7. It can be seen that the surface photocurrent increase obviously for all samples with the increasing HCHO concentrations.

To clearly observe the gas response of samples, the sensor response of In_2O_3-sensitized ZnO samples are calculated and shown in Fig. 8. The sensor response is defined as $[\{(I_b - I_a)/I_a\} \times 100\%]$, where I_a is the photocurrent in air and I_b is the photocurrent in the presence of HCHO. It was found that with the increasing of the HCHO concentrations, the sensor response of all In_2O_3-sensitized ZnO samples showed a linear increased. Different from the results of surface photocurrent spectra (see Fig. 5), the sample washed twice with $In(NO_3)_3$ aqueous solution (ZNFI-2 sample) presents the highest gas response. The response is ~19%, 90%, 189%, 270%, 347% and 419% corresponding to formaldehyde concentrations of ~5, 20, 40, 60, 80 and 100 ppm in the chamber, respectively. In particular, its response is more than 5 times larger than that of pure ZnO. Compared with the photoelectric gas sensors reported up to now,[27] this response value is relative high. These results indicate that the addition of In_2O_3 is beneficial to the HCHO sensing performance for ZnO sensors. Furthermore, the above results reveal that the sensitivity of sensor is relevant not only to the generation and transport processes of the photo-generated charge carriers but also the surface properties of the materials itself. On the one hand, with the increase in amount of In_2O_3 nanoparticles, the carrier concentration is increased. Correspondingly, the stronger photocurrent signal was observed. On the other hand, it is well known that the reaction of the sensor and the gas molecules takes place on the surface of the sensitive materials. When the amount of the sensitizers is added too much, In_2O_3 particles might be seriously agglomerate. This leads to a decrease in the number of the active sites on the surface of ZnO. Correspondingly, the number of oxygen ions chemisorbing will be reduced, resulting in the decrease of the gas response for In_2O_3-sensitized ZnO samples. The process of gas-sensing can be described as follows: in In_2O_3–ZnO composite systems, In_2O_3 nanoparticles served as the visible-light harvester, photo-generated electron producers and donators, while ZnO works as the gas-sensing unit, photo-generated electron acceptor and pathway for electrons transfer. When In_2O_3-sensitized ZnO sensors are irradiated by 460 nm light, the photo-generated electrons would be excited from the valence band of In_2O_3 to the conducting band firstly.

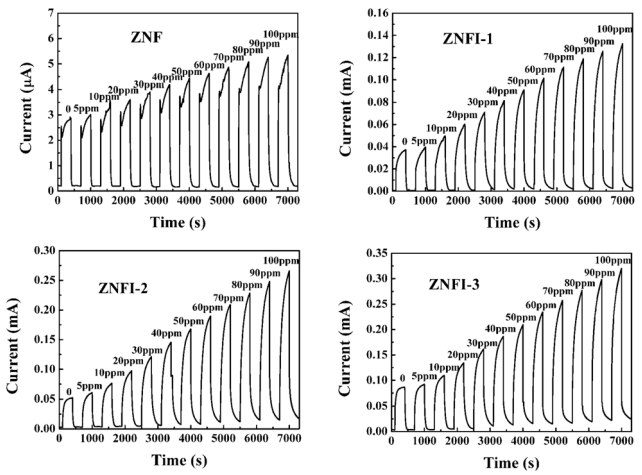

Fig. 7 The gas sensing response cycles of the ZnO and In_2O_3-sensitized ZnO nanoflowers to different concentrations of formaldehyde with a bias voltage of 10 V under 460 nm light irradiation.

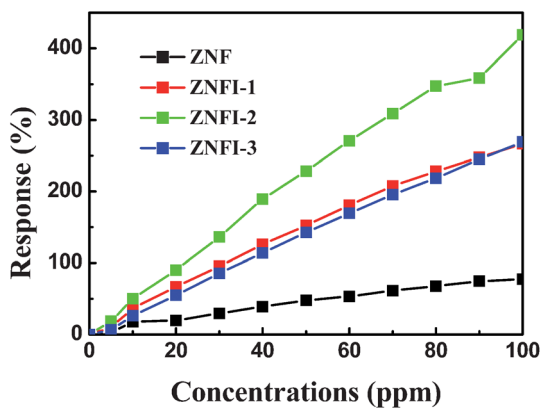

Fig. 8 The gas responses of the ZnO and In_2O_3-sensitized ZnO nanoflowers to various concentrations HCHO with a bias voltage of 10 V under 460 nm light irradiation.

The electrons then migrate to the surface of ZnO. The atmospheric oxygen molecules adsorbed on the samples' surface capture a certain amount of free electrons from the In_2O_3-sensitized ZnO samples and form various oxygen ions on the surface of ZnO.[50,51] When HCHO is introduced into the measurement chamber, it reacts with the oxygen species to form CO_2 and H_2O and the electrons captured by oxygen will be re-released which eventually increases the conductivity of In_2O_3-sensitized ZnO sensor.[8,52] As a result, the visible light detection for formaldehyde gas at room temperature was realized.

4. Conclusions

In summary, gas sensors based on In_2O_3-sensitized flowerlike ZnO have been prepared by a facile two-step process. The results of XRD, SEM and optical absorption reveal that In_2O_3 nanoparticles have coated on the surface of ZnO successfully and extend the absorption area from UV to vis. The sample that was washed twice with $In(NO_3)_3$ aqueous solution exhibited excellent sensitivity to HCHO under 460 nm visible light irradiation at room temperature. The response to 5 ppm HCHO can arrive to 19%. When the HCHO concentrations of test chamber reached 100 ppm, the response is up to 419%. The reason for this enhanced sensitivity is considered to be that the composite of In_2O_3–ZnO can improve the absorption to visible light and inhibit the recombination of electron–hole pairs to some extent, which can improve the sensing response.

Acknowledgements

For financial support, we are grateful to the National Natural Science Foundation of China (nos 21173103 and 51172090) and the Scientific Fore-front and Interdisciplinary Innovation Project, Jilin University, China (421031401412).

Notes and references

1 F. Rock, N. Barsan and U. Weimar, *Chem. Rev.*, 2008, **108**, 705–725.
2 G. Eranna, B. C. Joshi, D. P. Runthala and R. P. Gupta, *Crit. Rev. Solid State Mat. Sci.*, 2004, **29**, 111–188.
3 E. Oha, Ho. Y. Choib, S. H. Jungc, S. Choc, J. C. Kima, K. H. Leec, S. W. Kangd, J. Kimd and J. Y. Yund, *Sens. Actuators, B*, 2009, **141**, 239–243.
4 K. V. Gurav, P. R. Deshmukh and C. D. Lokhande, *Sens. Actuators, B*, 2011, **151**, 365–369.
5 A. Kolmakov, Y. Zhang, G. Cheng and M. Moskovits, *Adv. Mater.*, 2003, **15**, 997–1000.
6 D. Calestani, R. Mosca, M. Zanichelli, M. Villani and A. Zappettini, *J. Mater. Chem.*, 2011, **21**, 15532–15536.
7 H. S. Ahn, Y. Q. Wang, S. H. Jee, M. Park, Y. S. Yoon and D. J. Kim, *Chem. Phys. Lett.*, 2011, **511**, 331–335.
8 X. S. Fang, L. F. Hu, C. H. Ye and L. D. Zhang, *Pure Appl. Chem.*, 2010, **82**, 2185–2198.
9 S. Mishra, C. Ghanshyama, N. Rama, R. P. Bajpai and R. K. Bedi, *Sens. Actuators, B*, 2004, **97**, 387–390.
10 E. Comini, A. Cristalli, G. Faglia and G. Sberveglieri, *Sens. Actuators, B*, 2000, **65**, 260–263.
11 B. M. Wen, Y. Z. Huang and J. J. Boland, *J. Phys. Chem. C*, 2008, **112**, 106–111.
12 G. Y. Lu, J. Xu, J. B. Sun, Y. S. Yu, Y. Q. Zhang and F. M. Liu, *Sens. Actuators, B*, 2012, **162**, 82–88.
13 Y. M. Gui, S. M. Li, J. Q. Xu and C. Li, *Microelectron. J.*, 2008, **39**, 1120–1125.
14 J. Gong, Y. H. Li, X. S. Chai, Z. S. Hu and Y. L. Deng, *J. Phys. Chem. C*, 2010, **114**, 1293–1298.
15 N. V. Kaneva, D. T. Dimitrov and C. D. Dushkin, *Appl. Surf. Sci.*, 2011, **257**, 8113–8120.
16 L. Peng, D. Wang, M. Yang, T. Xie and Q. Zhao, *Appl. Surf. Sci.*, 2008, **254**, 2856–2860.
17 L. Peng, Q. Zhao, D. Wang, J. Zhai, P. Wang, S. Pang and T. Xie, *Sens. Actuators, B*, 2009, **136**, 80–85.
18 L. Peng, T.-F. Xie, M. Yang, P. Wang, D. Xu, S. Pang and D.-J. Wang, *Sens. Actuators, B*, 2008, **131**, 660–664.
19 L. Peng, P. Qin, Q. Zeng, H. Song, M. Lei, J. J. N. Mwangi, D. Wang and T. Xie, *Sens. Actuators, B*, 2011, **160**, 39–45.
20 G. Lu, J. Xu, J. Sun, Y. Yu, Y. Zhang and F. Liu, *Sens. Actuators, B*, 2012, **162**, 82–88.
21 Y. Gui, S. Li, J. Xu and C. Li, *Microelectron. J.*, 2008, **39**, 1120–1125.
22 M. Asilturk, F. Sayilkan and E. Arpac, *J. Photochem. Photobiol., A*, 2009, **203**, 64–71.
23 X. Q. Li, Y. Cheng, S. Z. Kang and J. Mu, *Appl. Surf. Sci.*, 2010, **256**, 6705–6709.
24 M. Yang, D. J. Wang, L. Peng, Q. D. Zhao, Y. H. Lin and X. Wei, *Sens. Actuators, B*, 2006, **117**, 80–85.
25 J. H. Park, O. O. Park and S. Kim, *Appl. Phys. Lett.*, 2006, **89**, 163106.
26 P. Sathishkumar, R. Sweena, J. Jerry and S. Anandan, *Chem. Eng. J.*, 2011, **171**, 136–140.
27 J. L. Zhai, D. J. Wang, L. Peng, Y. H. Lin, X. Y. Li and T. F. Xie, *Sens. Actuators, B*, 2010, **147**, 234–240.
28 R. Vogel, P. Hoyer and H. Weller, *J. Phys. Chem.*, 1994, **98**, 3183–3188.
29 G. L. Fan, W. Sun, H. Wang and F. Li, *Chem. Eng. J.*, 2011, **174**, 467–474.
30 J. K. Mishraa, S. Bhuniab, S. Banerjeea and P. Banerjia, *J. Lumin.*, 2008, **128**, 1169–1174.
31 X. D. Yan, C. W. Zou, X. D. Gao and W. Gao, *J. Mater. Chem.*, 2012, **22**, 5629–5640.
32 Y. Wang, W. Z. Jia, T. Strout, A. Schempf, H. Zhang, B. K. Li, J. H. Cui and Y. Lei, *Electroanalysis*, 2009, **21**(12), 1432–1438.
33 S. F. Chen, X. L. Yu, H. Y. Zhang and W. Liu, *J. Hazard. Mater.*, 2010, **180**, 735–740.
34 B. Yaglioglu, Y. J. Huang, H. Y. Yeom and D. C. Paine, *Thin Solid Films*, 2006, **496**, 89–94.
35 I. G. Benjaram, M. Reddy and A. Khan, *Appl. Catal., A*, 2003, **248**, 169–180.
36 Y. S. Song, J. K. Park, T. W. Kim and C. W. Chung, *Thin Solid Films*, 2004, **467**, 117–120.
37 D.-H. Shin, Y.-H. Kim, J.-W. Han, K.-M. Moon and R.-I. Murakami, *Trans. Nonferrous Met. Soc. China*, 2009, **19**(4), 997–1000.
38 B. Yaglioglu, H. Y. Yeom, R. Beresford and D. C. Paine, *Appl. Phys. Lett.*, 2006, **89**, 062103.
39 F. L. Zhou, X. J. Li, J. Shu and J. S. Wang, *J. Photochem. Photobiol., A*, 2011, **219**, 132–138.
40 Z. Y. Wang, B. B. Huang, Y. Dai, X. Y. Qin, X. Y. Zhang, P. Wang, H. X. Liu and J. X. Yu, *J. Phys. Chem. C*, 2009, **113**, 4612–4617.
41 Y. Zeng, T. Zhang, L. J. Wang and R. Wang, *J. Phys. Chem. C*, 2009, **113**, 3442–3448.
42 J. X. Wang, B. Zou, S. P. Ruan, J. Zhao and F. Q. Wu, *Mater. Chem. Phys.*, 2009, **117**, 489–493.
43 H. Gong, J. Q. Hu, J. H. Wang, C. H. Ong and F. R. Zhu, *Sens. Actuators, B*, 2006, **115**, 247–251.
44 P. Hu, N. Han, X. Zhang, M. S. Yao, Y. B. Cao, A. Zuo, G. Yang and F. L. Yuan, *J. Mater. Chem.*, 2011, **21**, 14277–14284.
45 Y. X. Wang, X. Y. Li, G. Lu, G. H. Chen and Y. Y. Chen, *Mater. Lett.*, 2008, **62**, 2359–2362.
46 Z. Fang, K. B. Tang, G. Z. Shen, D. Chen, R. Kong and S. J. Lei, *Mater. Lett.*, 2006, **60**, 2530–2533.
47 Q. D. Zhao, D. J. Wang, L. Peng, Y. H. Lin, M. Yang and T. F. Xie, *Chem. Phys. Lett.*, 2007, **434**, 96–100.
48 L. Peng, T. F. Xie, M. Yang, D. Xu, S. Pang and D. J. Wang, *Sens. Actuators, B*, 2008, **131**, 660–664.
49 Z. Y. Wang, B. B. Huang, Y. Dai, X. Y. Qin, X. Y. Zhang, P. Wang, H. X. Liu and J. X. Yu, *J. Phys. Chem. C*, 2009, **113**, 4612–4617.
50 C. C. Lin, S. Y. Chen, S. Y. Cheng and H. Y. Lee, *Appl. Phys. Lett.*, 2004, **84**, 5040–5042.
51 M. Law, H. Kind, B. Messer, F. Kim and P. Yang, *Angew. Chem., Int. Ed.*, 2002, **41**, 2405–2407.
52 D. S. Muggli, J. T. McCue and J. L. Falconer, *J. Catal.*, 1998, **173**, 470–483.

